ACCOUNTS of chemical research

Article

Cite This: Acc. Chem. Res. 2019, 52, 1485−1495

pubs.acs.org/accounts

Transistor-like Ultra-pH-Sensitive Polymeric Nanoparticles

Published as part of the Accounts of Chemical Research special issue "Nanomedicine and Beyond".

Qiang Feng, Jonathan Wilhelm, and Jinming Gao*

Harold C. Simmons Comprehensive Cancer Center, University of Texas Southwestern Medical Center, 6001 Forest Park Road, Dallas, Texas 75390, United States

CONSPECTUS: Electronic transistors have revolutionized the fields of microelectronics, computers, and mobile devices. Their ability to digitize electronic signals allows high fidelity data transfer as well as formation of logic gates. Inspired by electronic transistors, transistor-like organic materials have been under intensive investigation to amplify biological signals in a broad range of applications such as biosensing, diagnostic imaging, and therapeutic delivery.

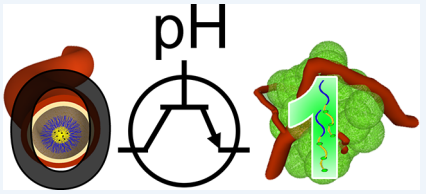

This Account highlights the inception and implementation of a "proton transistor" nanoparticle that can digitize acidotic pH signals in biological systems. Similar to electronic transistors, the ultra-pH-sensitive (UPS) nanoparticles derive their binary threshold response from phase separation phenomena. Hydrophobic micellization drives nanophase separation from unimers to aggregated polymeric micelles, which is responsible for the all-or-nothing proton distribution between the micelle and unimer states. Depending on the assembly status, conjugated fluorophores are quenched (micelle state) or freely fluoresce (solution unimer state) allowing robust detection of the phase transition behavior across a narrow pH range.

Based on this mechanistic insight, we created a UPS nanoparticle library encompassing a broad physiological pH range from 4.0 to 7.4. For biological applications, we engineered a barcode-like nanosensor capable of digitizing multiple pH signals at a single organelle resolution in live cells. The barcode system allowed easy identification of mutant Kirsten rat sarcoma viral oncogene (KRAS), a common mutation involved in tumorigenesis, which leads to rapid cellular proliferation, as the protein driver for accelerated organelle acidification and lysosome catabolism in a broad set of isogenic as well as heterogeneous cancer cell lines. Adoption of the technology to an ON−OFF/Always-ON design allowed the quantification of proton flux across the membranes of endocytic organelles. For medical applications, we demonstrate the ability to achieve binary detection of solid cancers with clear tumor margin delineation by near-infrared fluorescence imaging. Image-guided resection of head/neck and breast tumors resulted in significantly improved long-term survival over white light or tumor debulking surgeries in tumor-bearing mice, catapulting the clinical evaluation of the UPS nanosensor in cancer patients.

This Account serves as the first comprehensive summary of the molecular mechanism and biological applications of the digital pH threshold sensors. Building on the concept of cooperative phase transition behavior, we hope this Account will promote the rational design and development of additional transistor-like chemical sensors to digitize analog biological signals.

INTRODUCTION

The electronic transistor, first invented by Bardeen, Brattain, and Shockley in 1947 at Bell Laboratories, is recognized as one of the greatest inventions in the 20th century and has revolutionized the electronic, computer and mobile device industries.[1,2] An electronic transistor is a semiconductor device that can amplify or switch electronic signals, converting from analog inputs to digital outputs (0 or 1).[3] Signal digitization is able to maintain the high fidelity of original signals without signal distortion or noise introduction that are frequently encountered in the processing of analog signals.[4,5] Recently, polymeric semiconductor nanomaterials such as organic thin films have also been developed.[6−8] Beyond applications including active matrix display and radio frequency identification tags,[9,10] organic transistor-type nanomaterials have also emerged as biological or chemical sensors,[11,12] with special functionalization allowing stronger responses compared to conventional electrochemical sensors.[13] Developments in transistor-like material applications have emerged in an effort to digitize these processes for the design of simple circuits[14] or for use in therapeutic applications.[15] In the nanoparticle realm, recent development in stimuli-responsive materials has gained interest, leading to the production of liposomes that are responsive to heat[16] or light[17] as a payload release mechanism.[18] Recently, our lab has invented a series of ultra-pH-sensitive (UPS) nanoparticles[19−22] to amplify and digitize acidotic signals that are ubiquitous in biology.[23−26] A small perturbation of pH input signal (<0.3 pH) at a predetermined pH value was able to create a large increase in fluorescence output signal (>30-fold). In this Account, we discuss the molecular mechanism and implementation of these pH threshold nanoparticles to digitize acidotic signals in biology and medicine.

Received: February 15, 2019
Published: May 8, 2019

DOI: 10.1021/acs.accounts.9b00080
Acc. Chem. Res. 2019, 52, 1485−1495

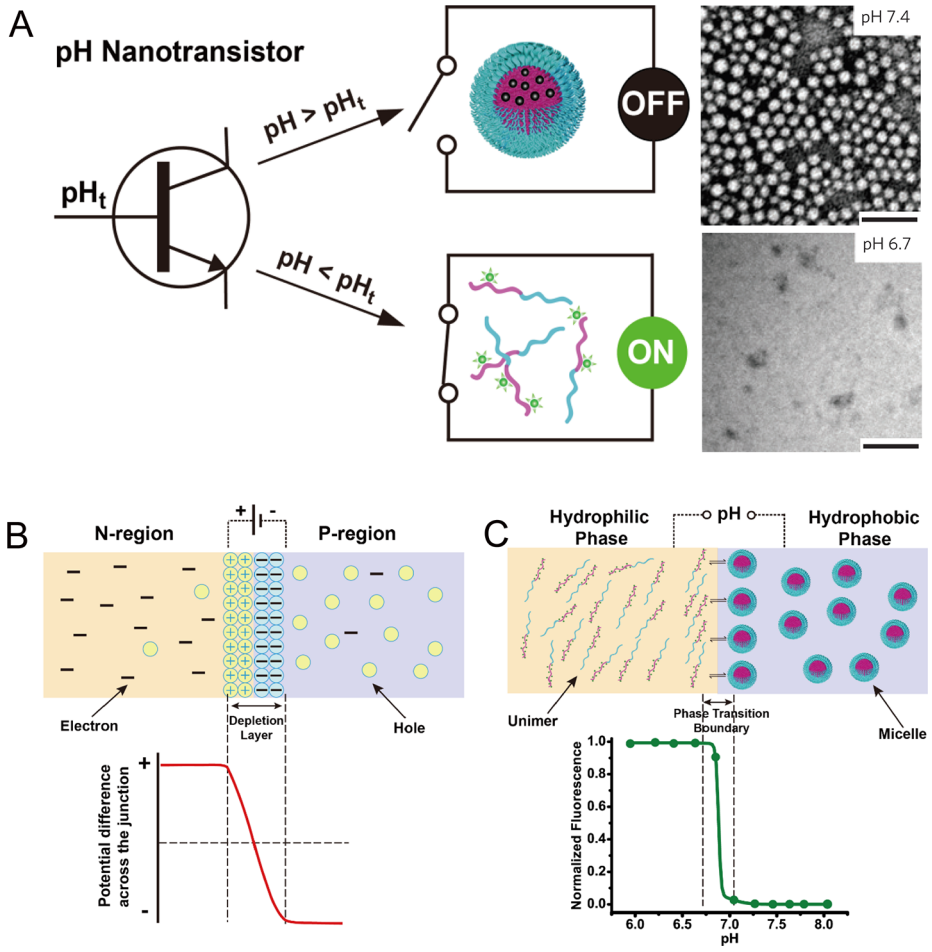

Figure 1. UPS nanoparticles exhibit similar signal switching behavior as an electronic transistor. (A) Schematic illustration and transmission electron microscopy image of the ON and OFF state of a representative pH nanosensor. The P/N junction of an electronic transistor (B) and UPS nanoparticles (C) derive their signal switching ability from phase separation phenomenon. Threshold voltage (V_t) and pH (pH_t) exist as gating indicators for electronic transistor and UPS nanoparticles, respectively. Binary on/off reporter signals (e.g., electric current or fluorescence intensity) can be achieved above or below the threshold values in each system. Reprinted with permission from ref 28. Copyright 2016 Nature Publishing Group.

pH THRESHOLD RESPONSE ARISES FROM PHASE SEPARATION

UPS nanoparticles can amplify acidotic signals across a threshold pH (pH_t). The transition between solution unimer phase and nanoscopic micelle phase results in large changes in fluorescence signal[19] and protonation status of the polymers.[27] In high pH environments ($pH > pH_t$), the fluorescent signals are abolished due to dye sequestration and quenching in the micelle core, representing the "off state". In the micellar state, the polymers are neutral in charge. At $pH < pH_t$, the unimers emit a fluorescent signal upon micelle disassembly, exhibiting the "on state". In the unimer state, a majority of the tertiary amine residues are protonated, giving each polymer chain a highly positive charge (Figure 1A). The ability of UPS nanoparticles to digitize acidotic signals is analogous to that of electronic transistors to shift electrical signals across a threshold voltage (Figure 1B).

The phase-modulated nanosensor displays a drastically different response to environmental pH compared to other types of pH sensors such as small molecular pH sensor (e.g., Lysosensor Green, Figure 2B,C), peptide-based pH sensor (e.g., pHLIP[29]), and other nanoparticle-based pH sensors (PEI, polylysine, and liposome).[27] The UPS nanoparticles produce a binary on−off signal response (Figure 2A). In contrast, the signal intensity generated by Lysosensor Green gradually increases as the pH drops. All the small molecular pH sensors we tested produce an analog signal response similar to Lysosensor Green. Similar to small molecular pH probes, the pHLIP peptides and other nanoparticle-based pH sensors all display a broad pH response unlike the UPS nanoparticles.

MOLECULAR COOPERATIVITY OF pH-INDUCED PHASE TRANSITION

We investigated the molecular pathway in the protonation/deprotonation process of the UPS nanoparticles (Figure 3A).[27] A flat pH plateau was detected during titration of the polymers, indicating strong buffer capacity. Dialysis and ^{1}H nuclear magnetic resonance (NMR) spectroscopy analysis during titration indicate that the polymers exhibit an all-or-nothing protonation behavior. Essentially, each micelle consists of multiple polymer chains and each polymer chain contains multiple tertiary amines, which can exhibit a protonated (positively charged) or deprotonated (neutral) state depending on the environmental pH. Along the majority of the titration coordinate, polymer chains are either highly protonated as unimers (all) or electrostatically neutral (nothing) inside

DOI: 10.1021/acs.accounts.9b00080
Acc. Chem. Res. 2019, 52, 1485−1495

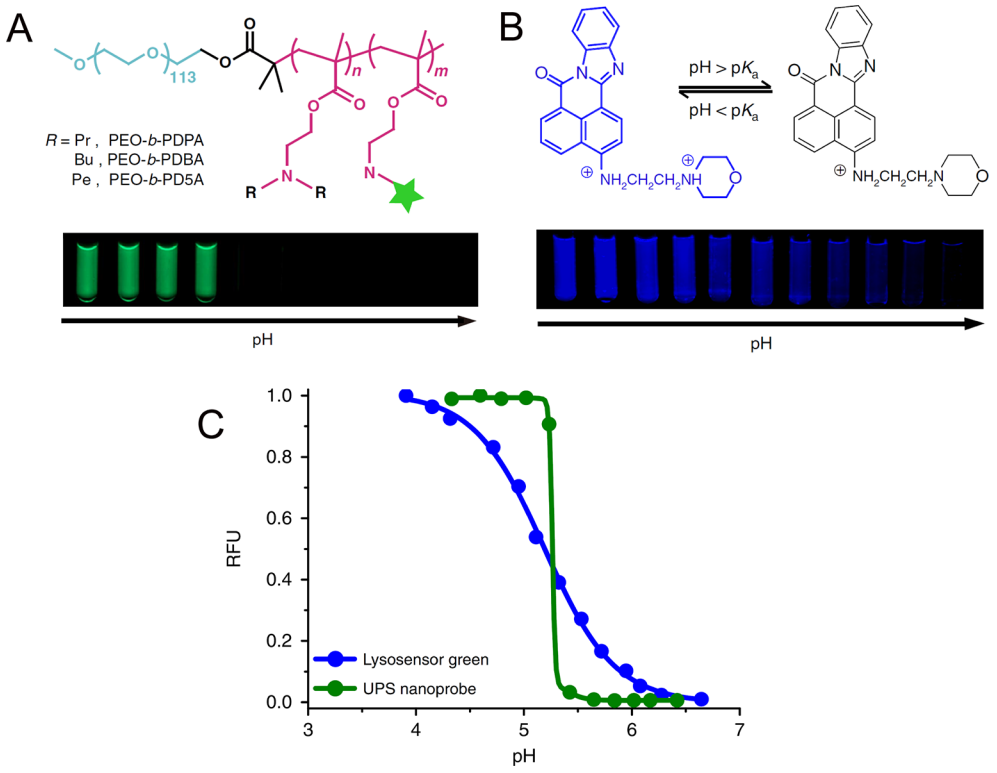

Figure 2. UPS nanosensor (A) and a small molecular pH sensor (B) display different signal response to the change of environmental pH. (C) A binary on/off response is observed with a representative UPS nanoprobe, whereas a gradual response is noted with Lysosensor Green. Reprinted with permission from refs 27 and 28 Copyright 2016 Nature Publishing Group.

micelles, with no partially protonated intermediate states in a single polymer chain. This all-or-nothing phenomenon is related to thermodynamics and critical micelle protonation degree (CMPD). Before self-assembly of the polymers into micelles can occur, the protonation degree of tertiary amines must fall below the CMPD, which is typically around 90% protonation for the poly(2-(diisopropylamino)ethyl methacrylate (PDPA) copolymer. Below CMPD, the hydrophobicity of the neutral tertiary amines drives phase separation and self-assembly of polymers into a charge-free micellar structure. Consequentially, this hydrophobicity-driven self-assembly lends an energetically favorable all-or-nothing protonation behavior to the polymer. Change in protonation degree of the overall system affects the molar distribution of the polymers between the two states. In contrast, most conventional pH responsive materials including small molecules such as NH_4Cl or chloroquine and macromolecules like polyethylenimine (PEI) or poly(L-lysine) (PLL) exhibit neither pH plateau nor all-or-nothing protonation behavior during titration. Rather than complete protonation of a subpopulation of the material, protonation occurs gradually among the conventional pH responsive polymers, where the average protonation degree is equivalent to the ratio of proton concentration over the initial tertiary amine concentration.

Proton NMR spectra of the alkyl protons adjacent to the nitrogen atom (e.g, a in Figure 3C) in deuterated water provide direct evidence of the divergent protonation state in the UPS unimer population (Figure 3B). During titration, the chemical shift of proton a in poly(ethylene oxide) (PEO)-*b*-PDPA remained constant while the integration of the corresponding peak decreased linearly, indicating that the protons distributed nonuniformly in an all or nothing behavior. In contrast, the chemical shift of proton a in PEO-*b*-poly(*N*,*N*-dimethylacrylamide) (PDMA) changed linearly while the integration of this peak remained constant along the titration coordinate, suggesting a homogeneous deprotonation process of the adjacent nitrogen. Of note, PEO-*b*-PDPA forms stable micelles after deprotonation, whereas PEO-*b*-PDMA remains in the unimer phase regardless of the environmental pH.

Experimental data demonstrate that cooperative deprotonation is driven by hydrophobic phase separation during micelle formation. Using an adopted allosteric model, Li et al.[27] generated the Hill plot of both cooperative and noncooperative systems. Quantitative analysis revealed that the PEO-*b*-PDPA exhibits strong positive cooperativity with a large Hill coefficient (n_H = 51). In contrast, materials that do not exhibit phase transition behavior (e.g., DPA monomer, PEO-*b*-PDMA, and PEI) have a Hill coefficient equal to or less than 1 (Figure 3D).

CREATION OF UPS NANOPARTICLE LIBRARY

The transition pH of the UPS nanoparticles can be precisely controlled by modulating the hydrophobicity of the PR segment of the polymer. Li et al. investigated the correlation between the hydrophobicity of the PR chains and the apparent pK_a or pH_t of the polymer in a physiological mimic environment with 150 mM NaCl.[30] The log *P* value (*P* is the partition coefficient of a solute between octanol and water, an indicator of hydrophobicity) of the monomer significantly affects the pH_t of the polymer: larger log *P* predicts lower pH_t of the nanosensor. Based on this insight, a random copolymerized PR block was introduced by varying the molar ratio of the two monomers to fine-tune the pH_t of the UPS nanoparticles to an operator-predetermined value.[31]

DOI: 10.1021/acs.accounts.9b00080
Acc. Chem. Res. 2019, 52, 1485−1495

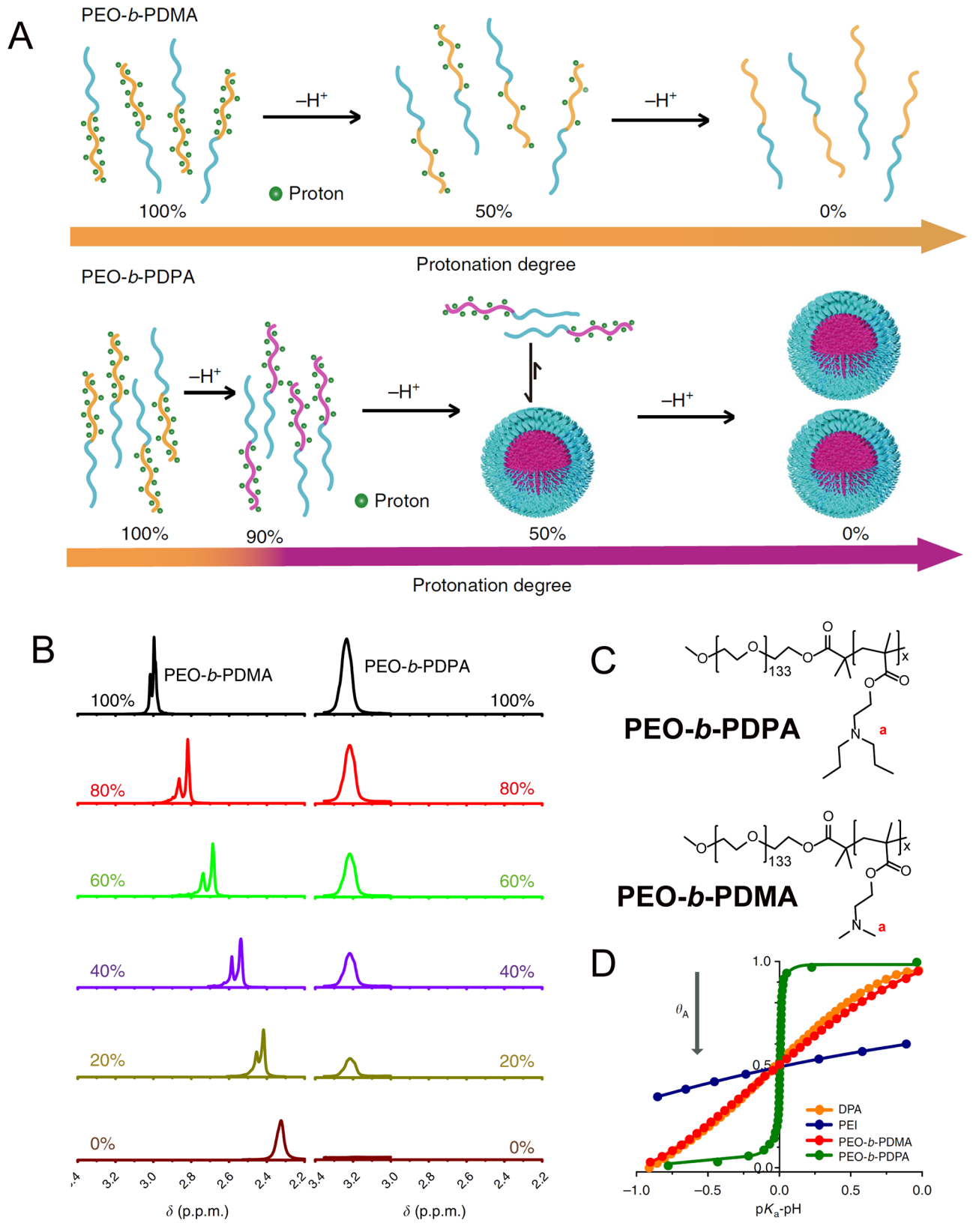

Figure 3. Cooperative deprotonation of tertiary ammonium groups driven by micelle assembly is essential for pH digitization. (A) PEO-*b*-PDMA, which does not form micelles, exhibits a gradual protonation state (top panel). PEO-*b*-PDPA exhibits a cooperative all-or-nothing protonation state, driven by micelle phase transition (bottom panel). (B) Proton NMR spectra (in D_2O) of alkyl protons (proton a in panel C) indicate gradual protonation of PEO-*b*-PDMA by linearly changing chemical shift with constant peak integration. In contrast, PEO-*b*-PDPA displays constant chemical shift with linearly decreasing peak integration, suggesting all-or-nothing protonation states. (D) PEO-*b*-PDPA displays strong cooperativity with a Hill coefficient of 51. DPA monomer, PEI, and PEO-*b*-PDMA do not exhibit cooperative behavior. Reprinted with permission from ref 27. Copyright 2016 Nature Publishing Group.

DOI: 10.1021/acs.accounts.9b00080
Acc. Chem. Res. 2019, 52, 1485−1495

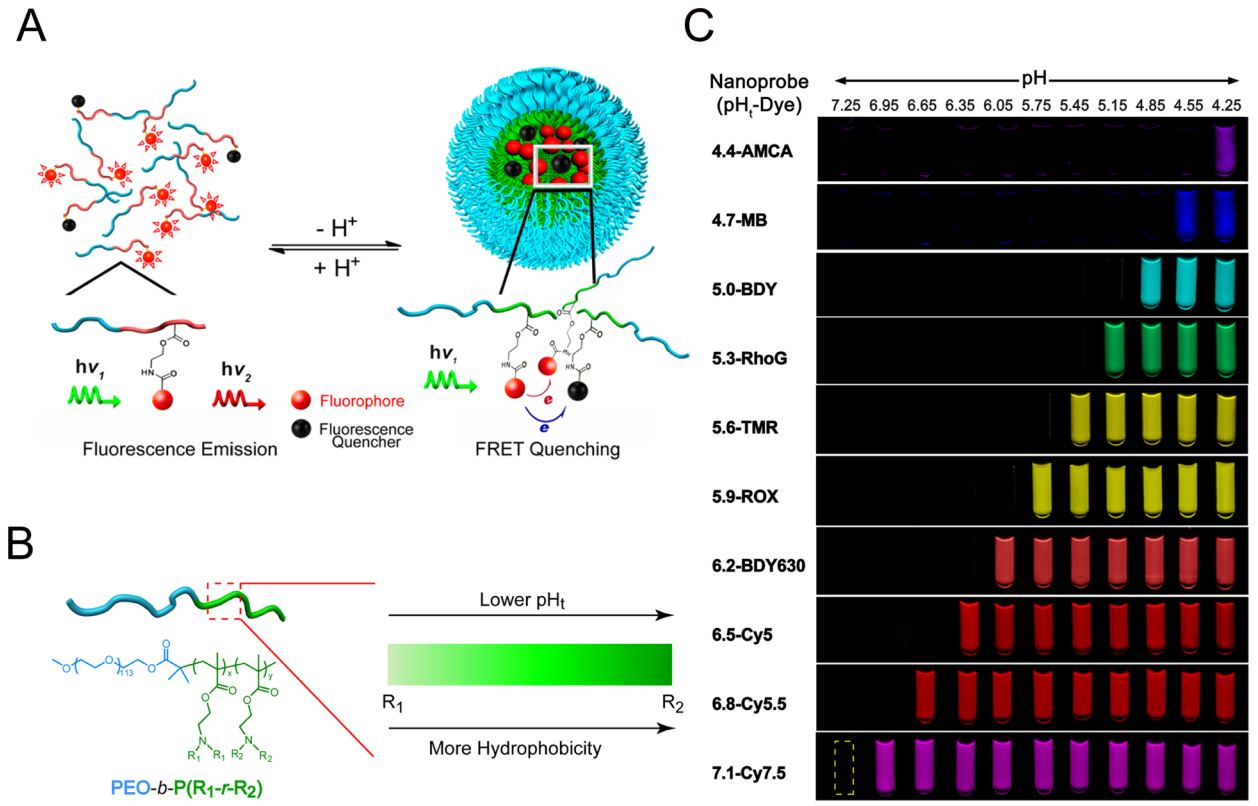

Figure 4. UPS nanoparticle library exhibits diverse pH and fluorescence tunability. (A) Schematic design of the on/off fluorescence signal activation as a result of pH-induced nanophase transition. (B) The pH_t of the nanosensor is controlled by varying the hydrophobicity of the PR region (ionizable tertiary amine block) of the polymer using a random copolymerization strategy. Higher hydrophobicity renders a lower transition pH. (C) A library of "proton transistor" sensors encode the broad pH range of 4−7.4 and emission from 400 to 820 nm. This library allows the digitization of pH in 0.3 increments. Reprinted with permission from ref 31. Copyright 2014 American Chemical Society.

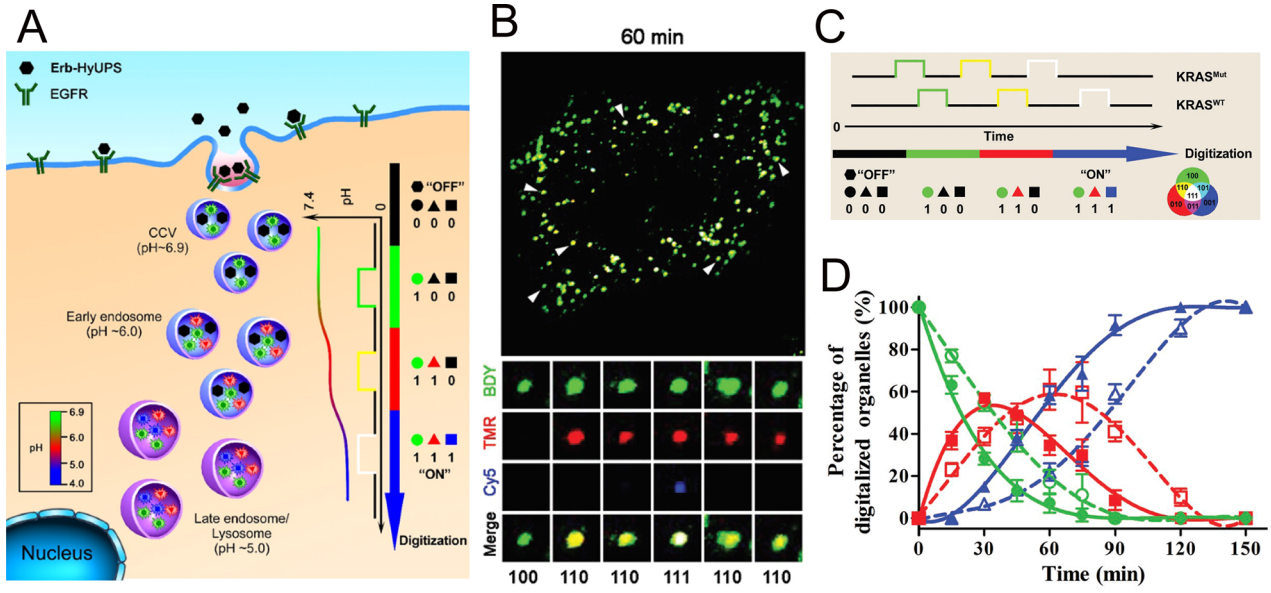

Figure 5. A digital barcode sensor for organelle pH measurement. (A) Schematic of barcode activation across different pH thresholds corresponding to different stages of organelle maturation. (B) The barcode sensor is capable of measuring endosomal pH at the single organelle level. (C, D) Cancer cells with KRAS mutation exhibit increased acidosis rates compared to KRAS wild type cells. Reprinted with permission from ref 41. Copyright 2017 Wiley-VCH Verlag GmbH & Co. KGaA, Weinheim.

For fluorescent sensor design, blackhole quenchers were incorporated in the system to allow for a wide selection of fluorophores with high on/off activation ratios across a small change in pH. The resulting nanosensor library is able to encode an entire range of physiological pH (4.0−7.4) through an emission spectrum from 400 to 820 nm (Figure 4).[31] The pH gap between on and off state of each individual probe is less than 0.3. This multichromatic UPS collection offers a

DOI: 10.1021/acs.accounts.9b00080
Acc. Chem. Res. 2019, 52, 1485−1495

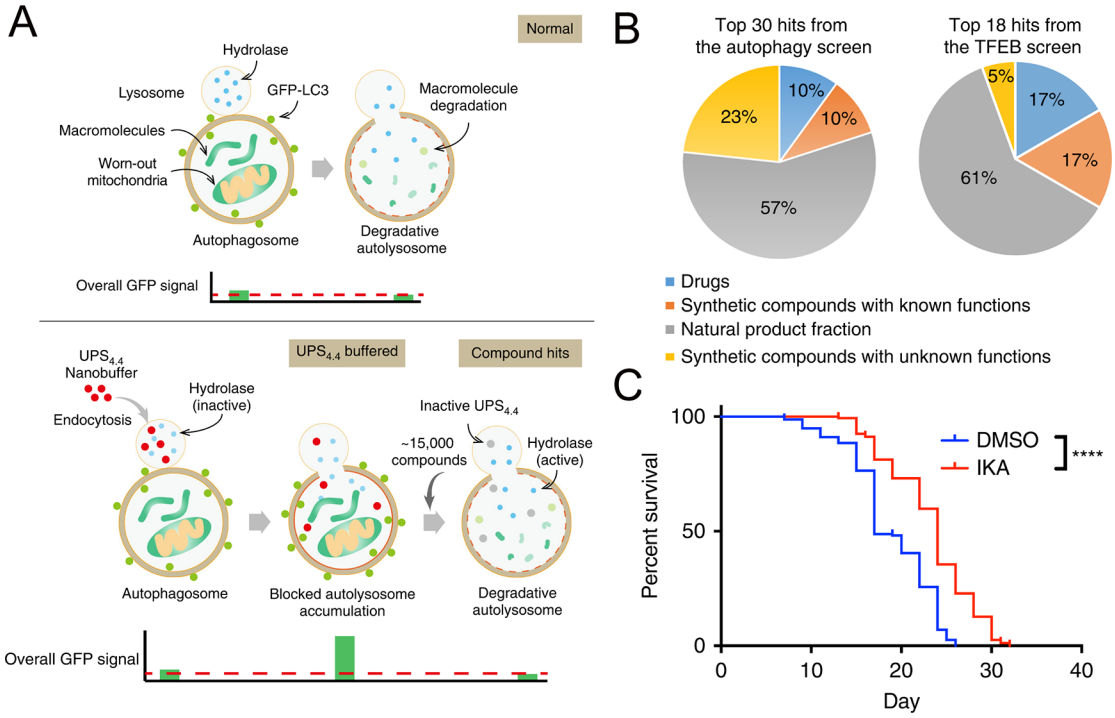

Figure 6. UPS nanoparticle-enabled high throughput screening of small molecular compounds that promote autophagolysosomal activity. (A) Conventional screening method (top) relies on GFP-LC3 degradation to determine autophagic flux promoted by various agents. pH buffering of autolysosomes by UPS platform extends the GFP imaging window for compound screening with reduced noise (bottom). (B) Screening of 18 000 compounds yielded a diverse pool of hit molecules. (C) Kaplan−Meier curves of *C. elegans* indicate that a TFEB agonist, ikarugamycin (IKA), improves survival compared to the control group treated with dimethyl sulfoxide (DMSO). Reprinted with permission from ref 44. Copyright 2016 Nature Publishing Group.

binary barcode library to digitize environmental pH based on the on/off status of multiple fluorescent emissions at specific pH thresholds.

DIGITIZATION OF LUMINAL pH OF ACIDIC ORGANELLES

Endosomes, lysosomes, and autolysosomes are acidic organelles inside cells. The pH gradient during organelle maturation plays an important role in receptor recycling, nutrient transport, and protein degradation.[32−34] Organelle acidification is also important for cell and immune signaling and antigen processing.[35−38] During the maturation process from early endosome to late endosome and to lysosome, the pH in the organelle lumen gradually decreases from 7.4 to 4.0. In the field of drug or gene delivery, the acidic lysosome is considered a major delivery barrier, responsible for degradation of the protein or nucleic acid drugs.[39,40] Elucidation of the organelle acidification process is of great importance in the study of cell physiology and design of drug delivery systems.

We produced a representative hybrid barcode nanosensor to digitize luminal pH of endocytic organelles at single organelle resolution (Figure 5).[41] The nanosensor is composed of three different polymer structures. The pH_t values of the three individual polymers are 6.9, 6.3, and 5.4, which encode for clathrin coated vesicles (CCVs), early endosomes, and late endosomes/lysosomes, respectively. Each polymer was conjugated with a unique fluorophore. At neutral pH, all three fluorescent dyes are quenched by either a homo-FRET or hetero-FRET mechanism, exhibiting a binary code as 0−0−0. When the organelle pH falls below 6.9, the 6.9 pH_t polymer is released from the micelles, resulting in the fluorescence activation of the 6.9 signal (encoded as 1−0−0). Upon an environment pH lower than 6.3, both the 6.9 and 6.3 signals are illuminated (1−1−0). After the organelle is acidified beyond a pH of 5.4, all of the fluorophores are activated, presenting the code as 1−1−1. By monitoring the activation status of each fluorescent channel over time, this probe digitizes the acidotic pH during organelle maturation. Using a series of isogenic cell lines with progressive mutations of P53, Kirsten rat sarcoma viral oncogene (KRAS) and LKB1 genes, the barcode sensor identified that the KRAS mutation was responsible for the accelerated organelle maturation and lysosome acidification, which is consistent with its role on increased macropinocytosis of albumin as a nutrient source for cancer cell growth and survival.[42] Using a modified on−off/always on nanosensor design, we further measured the acidification rate at 140−190 protons per second per organelle in HeLa cells, demonstrating the experimental feasibility to quantify proton flux across endosomal membranes.[43]

BUFFERING ORGANELLE pH FOR HIGH THROUGHPUT SCREENING

High concentrations of UPS nanoparticles (>400 μg/mL) can buffer luminal pH at different stages of organelle maturation. To investigate the biological consequences, HeLa cells were treated with different concentrations of UPS nanoparticles and the subsequent perturbations of cell signaling pathways were analyzed. Data identified a luminal pH threshold-dependent regulation of mTORC1 activity.[43] UPS nanoparticles with a buffering capacity above pH 5.0 were able to inhibit amino acid-dependent mTORC1 activation. In contrast, UPS nanoparticles with pH transition below 5.0 did not inhibit

DOI: 10.1021/acs.accounts.9b00080
Acc. Chem. Res. 2019, 52, 1485−1495

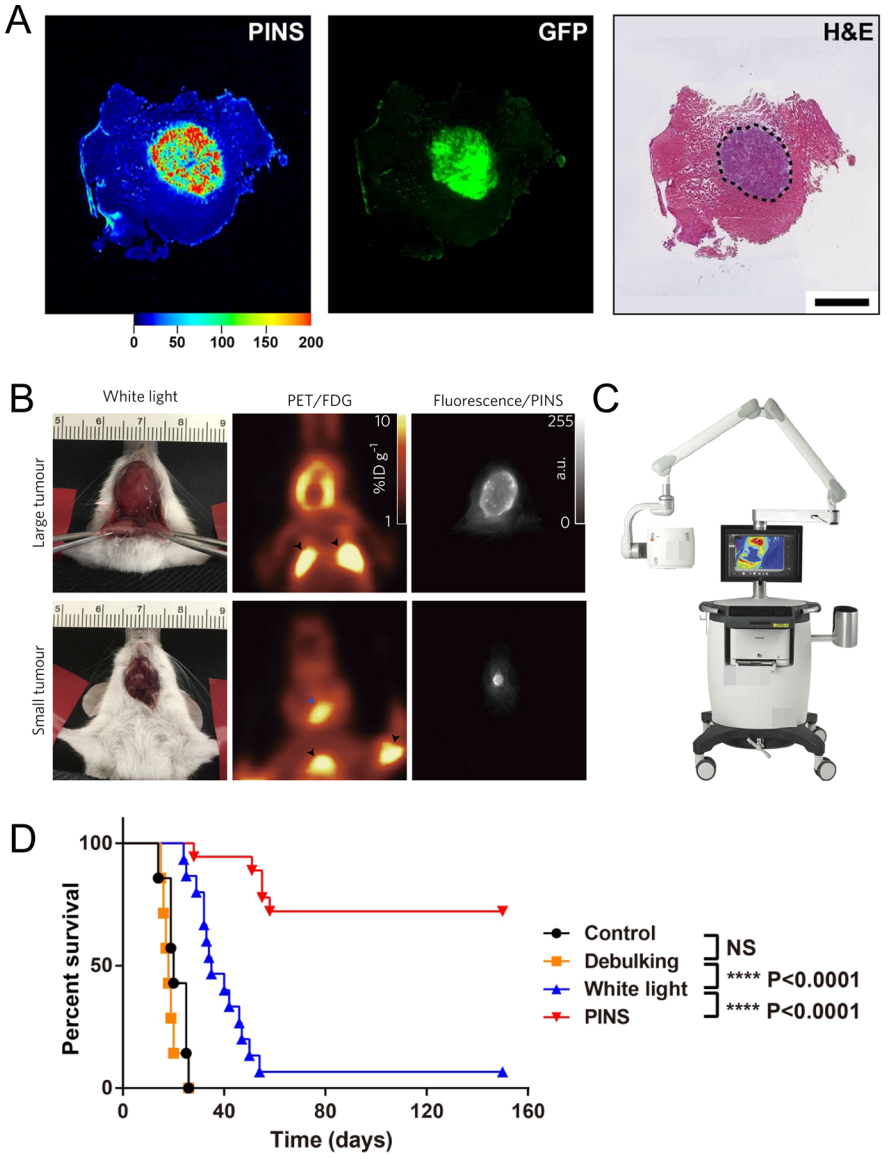

Figure 7. pH-activatable ICG-encoded nanosensor (PINS) illustrates binary tumor detection over surrounding muscle tissues. (A) The PINS probe can accurately depict the tumor margin as verified by H&E histology (dashed line). (B) The PINS probe offers conspicuous tumor detection over conventional FDG-PET imaging without false signals in tissues with high physiologic uptake of glucose. (C) Novadaq SPY Elite camera was used to image activated PINS signal in tumor-bearing mice. (D) Image-guided surgery using PINS significantly improves survival outcomes in mice compared to debulking or white light surgery. Reprinted with permission from ref 28. Copyright 2016 Nature Publishing Group.

mTORC1; however, they were able to delay the lysosomal degradation of albumin proteins.

Buffering organelle pH was employed to perform high throughput screening of small molecular compounds that accelerate autophagy and lysosome catabolism, which mimics starvation (Figure 6).[44] GFP-LC3 fusion proteins are commonly used as live cell markers for monitoring autophagic flux. GFP-LC3 forms punctate fluorescent pattern upon induction of autophagosomes, which are subsequently degraded in the autolysosomes. The innate autophagic flux makes it impossible to use GFP signals for high throughput applications. Upon treatment with UPS nanoparticles with a pH transition at 4.4, the autolysosomal pH was buffered to inhibit the degradation of GFP-LC3. This resulted in a 6-fold increase of GFP signal during live cell imaging, which enabled the phenotypic screen for small molecular compounds that can accelerate organelle acidification and protein degradation.

A UPS-enabled compound screen identified multiple drug or drug-like molecules including digoxin, ikarugamycin (IKA), and alexidine dihydrochloride that served as agonists for transcription factor EB (TFEB), a master regulator of autophagy and lysosome biogenesis.[45] The prospective compounds can robustly activate the TFEB pathway through three distinctive Ca^{2+} sources and Ca^{2+}-dependent mechanisms. In a diet-induced fatty liver disease mouse model, we found that these compounds effectively normalized lipid metabolism and overcame insulin-resistance. A survival study further confirmed that chemical activation of TFEB by ikarugamycin significantly prolonged the life span of *Caenorhabditis elegans*.[44]

DOI: 10.1021/acs.accounts.9b00080
Acc. Chem. Res. 2019, 52, 1485−1495

TUMOR IMAGING AND IMAGE-GUIDED CANCER SURGERY

Aerobic glycolysis, also known as the Warburg effect, represents a ubiquitous deregulated metabolism in a variety of cancer types.[46−48] Cancer cells preferentially take up glucose and convert it to lactic acid. The clinical manifestation of the Warburg effect is the broad use of ^{18}F-fluorodeoxyglucose (FDG) for noninvasive tumor diagnosis by positron emission tomography (PET). However, FDG-PET suffers from high false positive rates in tissues with high physiologic uptake of glucose (e.g., brain, brown fats). Excretion of metabolic acids and damaged lymphatic systems in solid cancers contribute to a persistent acidic tumor microenvironment.[49−52] Multiple pH responsive fluorescent or PET tracers have been designed for tumor imaging and diagnosis.[53−55] In most cases, these probes are effective at reporting the gradient pH values but are unable to provide clear tumor margin delineation with approximate binary output.

Transistor-like ultra-pH sensitive nanosensors display several advantages over traditional analog pH sensors, allowing for high fidelity imaging detection for tumor diagnosis and image-guided surgery. The binary signal output directly reports the pH status (higher or lower than a predetermined threshold) without external or internal references. In comparison, it is difficult to determine the pH status by analog probes without a standard curve as a reference. For UPS design, signal amplification aids in clear discrimination and simplification of complex biological environments.[19] The first pH-activatable nanoprobe design for *in vivo* tumor imaging employed Cy5.5-labeled nanoparticles.[21] The UPS_e is intended to accumulate in tumor tissues through the enhanced permeation and retention (EPR) effect and emit amplified signal of Cy5.5 in the acidic tumor microenvironment. The UPS_i is further modified with a cRGDfK peptide ligand to target angiogenic tumor vasculature with high expression of $\alpha_v\beta_3$ integrins. The resulting nanoprobe demonstrated robust cancer-specific imaging of solid tumors in a wide range of mouse tumor models including breast, prostate, head and neck, lung, brain, and pancreatic cancers.

Recently, the UPS_e probe was further modified to be compatible with clinical cameras for tumor imaging and image-guided cancer surgery.[28] The Cy5.5 dye in the previous design was replaced by indocyanine green (ICG), a clinically approved fluorophore, resulting in a sharper pH response, deeper tissue fluorescence penetration, and compatibility with multiple FDA-approved clinical cameras. This pH-activatable ICG-encoded nanosensor (PINS) has a relatively high efficiency targeting the tumor region (2−3% of the injected dose) and allows visualization of a variety of tumors with high signal-to-noise ratios. Sections of tumor and adjacent tissues clearly illustrate a discrete tumor margin delineation as verified by histology (Figure 7A). Compared to FDG-PET imaging, PINS probes generated conspicuous detection of large or small head and neck tumors without the false positive signals in tissues such as brown fats or tensed muscles exhibited by FDG-PET, demonstrating key benefits from digitization and amplification of biological signals (Figure 7B).

Accurate margin detection allows precise resection of tumors under image guidance. Real-time cancer surgeries in murine HN5 head and neck cancer model and 4T1 breast cancer model were performed using the SPY Elite system (Figure 7C), a camera widely used in operating rooms.[28] Even small residual tumor nodules (<1 million cells), which were invisible under white light, exhibited clear visualization, resulting in a more complete tumor resection. The long-term survival rate significantly increased (>70%) under PINS guidance compared with white light or debulking surgeries (Figure 7D).

SUMMARY AND FUTURE PERSPECTIVE

This Account summarizes the development of transistor-like ultra-pH-sensitive nanoparticles to digitize acidotic signals in biological systems. The original impetus of this work was to establish a pH-activatable nanocarrier capable of delivering therapeutic payloads inside mildly acidic endocytic organelles before reaching the more acidic, degradative lysosomes. Early work was inspired by research advances from many laboratories in drug and gene delivery.[56−61] After reviewing various design options, we decided to investigate the current ionizable polymeric system, hypothesizing that a lower energy barrier from noncovalent self-assembly would render faster kinetics and more cooperative response over covalent, pH-labile systems. This intuition was validated by the fast (milliseconds after pH activation) and sharp ($\Delta pH_{on/off}$ < 0.3) responses to subtle changes in the environmental pH.[19] Specific UPS compositions were further shown to differentiate early endosomal vs later endosomal pH in live cells. Over the ensuing years, we elucidated the molecular mechanism of the ultra-pH-sensitive response and identified nano-phase separation as the driving force for the all-or-nothing protonation phenotype that is absent in small molecular or common polymeric bases (e.g., polyethylenimine, polylysine, chitosan, etc.).[27] Inspired by the electronic transistor concept, we demonstrate the use of UPS nanoparticles as a "proton transistor" to digitize endocytic pH that allowed identification of mutant KRAS as an oncogenic driver for accelerated organelle maturation.[41] In addition, we illustrate the feasibility to achieve a binary delineation of tumor margins by fluorescence imaging and ability to improve the precision of cancer surgery (Figure 7), which propelled the clinical testing of the UPS nanosensor.

Moving forward, we envision several new lines of inquiry on the development and evaluation of the transistor concept at the chemical and biological interface. First, is it feasible to achieve additional digital outputs besides fluorescence as exemplified in this Account? Recent functionalization of the UPS nanoparticles with a positron emitter, ^{64}Cu, showed noninvasive detection of occult tumor nodules by positron emission tomography.[62] Autoradiography analysis of positron signals illustrated binary readouts of tumors over the surrounding tissues, indicating the possibility to extend signal digitization beyond fluorescence. Second, is it possible to define the structural requirement of polymers to achieve transistor-like ultrasensitive response? In our pursuit of biodegradable UPS systems, we discovered polymer backbones can greatly impact the sharpness of pH response. Several attempts using amide or peptide backbones failed to achieve an ultrasensitive response likely due to the restrained chain rotation and introduction of hydrogen bonds that disrupt the molecular dynamics of pH-induced self-assembly (data not published). Elucidating the structural constraints to allow cooperative phase transitions will be valuable to design new nanomaterials not only for sensing pH but also other stimuli of interest. Third, can UPS nanoparticle system be functionally expanded in the form of simple logic gates or a multiplexed barcode system? Maintaining the current fluorescence reporter of the nano-

DOI: 10.1021/acs.accounts.9b00080
Acc. Chem. Res. 2019, 52, 1485−1495

particle platform, a form of NOT gate could be achieved through a hetero-FRET mechanism (contrary to the current UPS design), lending additional logical information to users. For example, the NOT gate would provide surgeons with information on whether a negative signal is truly exhibiting a high pH environment or if it is caused by a lack of tissue perfusion. Through design of additional stimuli responses in the same nanoparticle (e.g., enzyme expression, reactive oxygen species), the platform could generate a multiplexed barcode, encoding more information than possible with the current pH-only reporter. Finally, can UPS nanoparticles and the related proton transistor concept deliver the anticipated impact in biological discovery and medicine? This Account highlighted the recent advances in investigating endosomal biology and improving cancer surgery in an academic setting. It remains to be seen whether these efforts can offer the ultimate value addition in drug development and patient care. While indocyanine green is clinically approved for intravenous administration and our preclinical studies show limited toxicity of UPS platform, many hurdles still exist in whether observations in tumor-bearing mice can translate into human patients, whether these particles will be safe for human use, and whether production and regulatory complexity will be cost prohibitive over traditional small molecular agents. On-going clinical trials of the UPS nanosensor in cancer surgery will provide the first "acid" test and offer useful lessons on translating an invention from the lab to the clinics.

AUTHOR INFORMATION

Corresponding Author

*E-mail: jinming.gao@utsouthwestern.edu.

ORCID

Qiang Feng: 0000-0002-3665-3914
Jinming Gao: 0000-0003-0726-5098

Author Contributions

J.G. initiated the outline of the account. Q.F. and J.W. wrote the first draft and created all the figures. J.G. revised and finalized the review. The authors give approval to the final version of the manuscript.

Notes

The authors declare the following competing financial interest(s): J.G. is a founder and scientific advisor for OncoNano Medicine, Inc.

Biographies

Qiang Feng received his B.S. (2012) and M.S. (2014) in pharmaceutics from Peking University and obtained a Ph.D. (2017) in nanoscience from National Center for Nanoscience and Technology, University of Chinese Academy of Sciences. He joined Dr. Jinming Gao's lab at UT Southwestern Medical Center as a postdoctoral fellow in August of 2017. His research interests are in the development and implementation of pH sensitive nanotechnology for tumor imaging and biological interrogation.

Jonathan Wilhelm received his B.S. (2017) in chemical engineering from Texas Tech University. He joined Dr. Jinming Gao's lab at UT Southwestern Medical Center as a graduate student in August of 2017. As a student in biomedical engineering, his research interests are in the development of peptide-loaded pH sensitive nanoparticles for immune-oncology applications.

Jinming Gao received his B.S. in chemistry from Peking University in 1991. He obtained his Ph.D. under Dr. George M. Whitesides in physical organic chemistry at Harvard University in 1996. His postdoctoral training was under Dr. Robert S. Langer in biomedical engineering at MIT. In 1998, he started his lab in the Department of Biomedical Engineering at Case Western Reserve University. In 2005, he moved to UT Southwestern Medical Center at Dallas, Texas, where he is holding the Robert B. and Virginia Payne Professorship in Oncology. His current research interests focus on the understanding of nanoscale cooperativity and its implementation in niche biomedical applications. The lab-invented proton threshold nanosensor entered first-in-human trials for image-guided cancer surgery in 2018.

ACKNOWLEDGMENTS

We appreciate the funding support from the National Institutes of Health (Grants R01CA192221, R01CA211930, and U01CA218422) and the Cancer Prevention Research Institute of Texas (RP180343). The lab is also supported by the Mendelson-Young Endowment in Cancer Therapeutics.

REFERENCES

(1) Bardeen, J. Research leading to point-contact transistor. *Science* **1957**, *126*, 105−112.
(2) Moore, G. E. Progress in digital integrated electronics. *Technol. Dig. - Int. Electron Devices Meet.* **1975**, 11.
(3) Heinrich, H.; Hemenway, B.; McGroddy, K.; Bloom, D. Measurement of real-time digital signals in a silicon bipolar junction transistor using a noninvasive optical probe. *Electron. Lett.* **1986**, *22*, 650−652.
(4) Goncharenko, I.; Esman, A.; Kuleshov, V.; Pilipovich, V. Optical analog signal digitization. *Meas. Tech.* **2007**, *50*, 916−920.
(5) Elliott, M. A.; Insko, E. K.; Greenman, R. L.; Leigh, J. S. Improved resolution and signal-to-noise ratio in MRI via enhanced signal digitization. *J. Magn. Reson.* **1998**, *130*, 300−304.
(6) Horowitz, G. Organic field-effect transistors. *Adv. Mater.* **1998**, *10*, 365−377.
(7) Facchetti, A.; Yoon, M. H.; Marks, T. J. Gate dielectrics for organic field-effect transistors: new opportunities for organic electronics. *Adv. Mater.* **2005**, *17*, 1705−1725.
(8) Franklin, A. D. Nanomaterials in transistors: From high-performance to thin-film applications. *Science* **2015**, *349*, aab2750.
(9) Steudel, S.; Myny, K.; Arkhipov, V.; Deibel, C.; De Vusser, S.; Genoe, J.; Heremans, P. 50 MHz rectifier based on an organic diode. *Nat. Mater.* **2005**, *4*, 597−600.
(10) Baude, P.; Ender, D.; Haase, M.; Kelley, T.; Muyres, D.; Theiss, S. Pentacene-based radio-frequency identification circuitry. *Appl. Phys. Lett.* **2003**, *82*, 3964−3966.
(11) Tang, H.; Yan, F.; Lin, P.; Xu, J. B.; Chan, H. L. W. Highly Sensitive Glucose Biosensors Based on Organic Electrochemical Transistors Using Platinum Gate Electrodes Modified with Enzyme and Nanomaterials. *Adv. Funct. Mater.* **2011**, *21*, 2264−2272.
(12) Park, J. W.; Park, S. J.; Kwon, O. S.; Lee, C.; Jang, J. Polypyrrole Nanotube Embedded Reduced Graphene Oxide Transducer for Field-Effect Transistor-Type H2O2 Biosensor. *Anal. Chem.* **2014**, *86*, 1822−1828.
(13) Wang, N.; Yang, A.; Fu, Y.; Li, Y.; Yan, F. Functionalized Organic Thin Film Transistors for Biosensing. *Acc. Chem. Res.* **2019**, *52*, 277−287.
(14) Bonnet, J.; Yin, P.; Ortiz, M. E.; Subsoontorn, P.; Endy, D. Amplifying genetic logic gates. *Science* **2013**, *340*, 599−603.
(15) Holt, B. A.; Kwong, G. A. Bacterial defiance as a form of prodrug failure. bioRxiv, 2019, https://www.biorxiv.org/content/10.1101/556951v1.
(16) Ta, T.; Porter, T. M. Thermosensitive liposomes for localized delivery and triggered release of chemotherapy. *J. Controlled Release* **2013**, *169*, 112−125.

DOI: 10.1021/acs.accounts.9b00080
Acc. Chem. Res. 2019, 52, 1485−1495

(17) Miranda, D.; Lovell, J. F. Mechanisms of Light-induced Liposome Permeabilization. *Bioeng. Transl. Med.* **2016**, *1*, 267−276.
(18) Torchilin, V. P. Recent advances with liposomes as pharmaceutical carriers. *Nat. Rev. Drug Discovery* **2005**, *4*, 145−160.
(19) Zhou, K.; Wang, Y.; Huang, X.; Luby-Phelps, K.; Sumer, B. D.; Gao, J. Tunable, Ultrasensitive pH-Responsive Nanoparticles Targeting Specific Endocytic Organelles in Living Cells. *Angew. Chem., Int. Ed.* **2011**, *50*, 6109−6114.
(20) Zhou, K.; Liu, H.; Zhang, S.; Huang, X.; Wang, Y.; Huang, G.; Sumer, B. D.; Gao, J. Multicolored pH-tunable and activatable fluorescence nanoplatform responsive to physiologic pH stimuli. *J. Am. Chem. Soc.* **2012**, *134*, 7803−7811.
(21) Wang, Y.; Zhou, K.; Huang, G.; Hensley, C.; Huang, X.; Ma, X.; Zhao, T.; Sumer, B. D.; DeBerardinis, R. J.; Gao, J. A nanoparticle-based strategy for the imaging of a broad range of tumours by nonlinear amplification of microenvironment signals. *Nat. Mater.* **2014**, *13*, 204−212.
(22) Huang, X.; Huang, G.; Zhang, S.; Sagiyama, K.; Togao, O.; Ma, X.; Wang, Y.; Li, Y.; Soesbe, T. C.; Sumer, B. D.; Takahashi, M.; Sherry, A. D.; Gao, J. Multi-Chromatic pH-Activatable ^{19}F-MRI Nanoprobes with Binary ON/OFF pH Transitions and Chemical-Shift Barcodes. *Angew. Chem., Int. Ed.* **2013**, *52*, 8074−8078.
(23) Gatenby, R. A.; Gillies, R. J. Why do cancers have high aerobic glycolysis? *Nat. Rev. Cancer* **2004**, *4*, 891.
(24) Neri, D.; Supuran, C. T. Interfering with pH regulation in tumours as a therapeutic strategy. *Nat. Rev. Drug Discovery* **2011**, *10*, 767−777.
(25) Cardone, R. A.; Casavola, V.; Reshkin, S. J. The role of disturbed pH dynamics and the Na+/H+ exchanger in metastasis. *Nat. Rev. Cancer* **2005**, *5*, 786−795.
(26) Waldmann, R.; Champigny, G.; Bassilana, F.; Heurteaux, C.; Lazdunski, M. A proton-gated cation channel involved in acid-sensing. *Nature* **1997**, *386*, 173−177.
(27) Li, Y.; Zhao, T.; Wang, C.; Lin, Z.; Huang, G.; Sumer, B. D.; Gao, J. Molecular basis of cooperativity in pH-triggered supramolecular self-assembly. *Nat. Commun.* **2016**, *7*, 13214.
(28) Zhao, T.; Huang, G.; Li, Y.; Yang, S.; Ramezani, S.; Lin, Z.; Wang, Y.; Ma, X.; Zeng, Z.; Luo, M.; de Boer, E.; Xie, X. J.; Thibodeaux, J.; Brekken, R. A.; Sun, X.; Sumer, B. D.; Gao, J. A Transistor-like pH Nanoprobe for Tumour Detection and Image-guided Surgery. *Nat. Biomed. Eng.* **2016**, *1*, 0006.
(29) Anderson, M.; Moshnikova, A.; Engelman, D. M.; Reshetnyak, Y. K.; Andreev, O. A. Probe for the measurement of cell surface pH in vivo and ex vivo. *Proc. Natl. Acad. Sci. U. S. A.* **2016**, *113*, 8177−8181.
(30) Li, Y.; Wang, Z.; Wei, Q.; Luo, M.; Huang, G.; Sumer, B. D.; Gao, J. Non-covalent interactions in controlling pH-responsive behaviors of self-assembled nanosystems. *Polym. Chem.* **2016**, *7*, 5949−5956.
(31) Ma, X.; Wang, Y.; Zhao, T.; Li, Y.; Su, L. C.; Wang, Z.; Huang, G.; Sumer, B. D.; Gao, J. Ultra-pH-sensitive nanoprobe library with broad pH tunability and fluorescence emissions. *J. Am. Chem. Soc.* **2014**, *136*, 11085−11092.
(32) Maxfield, F. R.; McGraw, T. E. Endocytic recycling. *Nat. Rev. Mol. Cell Biol.* **2004**, *5*, 121−132.
(33) Luzio, J. P.; Pryor, P. R.; Bright, N. A. Lysosomes: fusion and function. *Nat. Rev. Mol. Cell Biol.* **2007**, *8*, 622−632.
(34) Saftig, P.; Klumperman, J. Lysosome biogenesis and lysosomal membrane proteins: trafficking meets function. *Nat. Rev. Mol. Cell Biol.* **2009**, *10*, 623−635.
(35) Ip, W. K. E.; Sokolovska, A.; Charriere, G. M.; Boyer, L.; Dejardin, S.; Cappillino, M. P.; Yantosca, L. M.; Takahashi, K.; Moore, K. J.; Lacy-Hulbert, A.; Stuart, L. M. Phagocytosis and Phagosome Acidification Are Required for Pathogen Processing and MyD88-Dependent Responses to Staphylococcus aureus. *J. Immunol.* **2010**, *184*, 7071−7081.
(36) Harding, C. V.; Collins, D. S.; Slot, J. W.; Geuze, H. J.; Unanue, E. R. Liposome-encapsulated antigens are processed in lysosomes, recycled, and presented to T cells. *Cell* **1991**, *64*, 393−401.
(37) Savina, A.; Jancic, C.; Hugues, S.; Guermonprez, P.; Vargas, P.; Moura, I. C.; Lennon-Dumenil, A. M.; Seabra, M. C.; Raposo, G.; Amigorena, S. NOX2 controls phagosomal pH to regulate antigen processing during crosspresentation by dendritic cells. *Cell* **2006**, *126*, 205−218.
(38) Huotari, J.; Helenius, A. Endosome maturation. *EMBO J.* **2011**, *30*, 3481−3500.
(39) Rabinow, B. E. Nanosuspensions in drug delivery. *Nat. Rev. Drug Discovery* **2004**, *3*, 785−796.
(40) Torchilin, V. P. Multifunctional, stimuli-sensitive nanoparticulate systems for drug delivery. *Nat. Rev. Drug Discovery* **2014**, *13*, 813−827.
(41) Wang, Y.; Wang, C.; Li, Y.; Huang, G.; Zhao, T.; Ma, X.; Wang, Z.; Sumer, B. D.; White, M. A.; Gao, J. Digitization of Endocytic pH by Hybrid Ultra-pH-Sensitive Nanoprobes at Single-Organelle Resolution. *Adv. Mater.* **2017**, *29*, 1603794.
(42) Commisso, C.; Davidson, S. M.; Soydaner-Azeloglu, R. G.; Parker, S. J.; Kamphorst, J. J.; Hackett, S.; Grabocka, E.; Nofal, M.; Drebin, J. A.; Thompson, C. B.; Rabinowitz, J. D.; Metallo, C. M.; Vander Heiden, M. G.; Bar-Sagi, D. Macropinocytosis of protein is an amino acid supply route in Ras-transformed cells. *Nature* **2013**, *497*, 633.
(43) Wang, C.; Wang, Y.; Li, Y.; Bodemann, B.; Zhao, T.; Ma, X.; Huang, G.; Hu, Z.; DeBerardinis, R. J.; White, M. A.; Gao, J. A nanobuffer reporter library for fine-scale imaging and perturbation of endocytic organelles. *Nat. Commun.* **2015**, *6*, 8524.
(44) Wang, C.; Niederstrasser, H.; Douglas, P. M.; Lin, R.; Jaramillo, J.; Li, Y.; Oswald, N. W.; Zhou, A.; McMillan, E. A.; Mendiratta, S.; Wang, Z.; Zhao, T.; Lin, Z.; Luo, M.; Huang, G.; Brekken, R. A.; Posner, B. A.; MacMillan, J. B.; Gao, J.; White, M. A. Small-molecule TFEB pathway agonists that ameliorate metabolic syndrome in mice and extend C. elegans lifespan. *Nat. Commun.* **2017**, *8*, 2270.
(45) Settembre, C.; Di Malta, C.; Polito, V. A.; Arencibia, M. G.; Vetrini, F.; Erdin, S.; Erdin, S. U.; Huynh, T.; Medina, D.; Colella, P.; Sardiello, M.; Rubinsztein, D. C.; Ballabio, A. TFEB Links Autophagy to Lysosomal Biogenesis. *Science* **2011**, *332*, 1429−1433.
(46) Vander Heiden, M. G.; Cantley, L. C.; Thompson, C. B. Understanding the Warburg effect: the metabolic requirements of cell proliferation. *Science* **2009**, *324*, 1029−1033.
(47) Kim, J. W.; Dang, C. V. Cancer's molecular sweet tooth and the Warburg effect. *Cancer Res.* **2006**, *66*, 8927−8930.
(48) Koppenol, W. H.; Bounds, P. L.; Dang, C. V. Otto Warburg's contributions to current concepts of cancer metabolism. *Nat. Rev. Cancer* **2011**, *11*, 325−337.
(49) Vaupel, P.; Kallinowski, F.; Okunieff, P. Blood-Flow, Oxygen and Nutrient Supply, and Metabolic Microenvironment of Human-Tumors - a Review. *Cancer Res.* **1989**, *49*, 6449−6465.
(50) Fukumura, D.; Jain, R. K. Tumor microenvironment abnormalities: Causes, consequences, and strategies to normalize. *J. Cell. Biochem.* **2007**, *101*, 937−949.
(51) Hsu, P. P.; Sabatini, D. M. Cancer cell metabolism: Warburg and beyond. *Cell* **2008**, *134*, 703−707.
(52) Corbet, C.; Feron, O. Tumour acidosis: from the passenger to the driver's seat. *Nat. Rev. Cancer* **2017**, *17*, 577−593.
(53) Duan, Q. P.; Cao, Y.; Li, Y.; Hu, X. Y.; Xiao, T. X.; Lin, C.; Pan, Y.; Wang, L. Y. pH-Responsive Supramolecular Vesicles Based on Water-Soluble Pillar[6]arene and Ferrocene Derivative for Drug Delivery. *J. Am. Chem. Soc.* **2013**, *135*, 10542−10549.
(54) Flavell, R. R.; Truillet, C.; Regan, M. K.; Ganguly, T.; Blecha, J. E.; Kurhanewicz, J.; VanBrocklin, H. F.; Keshari, K. R.; Chang, C. J.; Evans, M. J.; Wilson, D. M. Caged [F-18]FDG Glycosylamines for Imaging Acidic Tumor Microenvironments Using Positron Emission Tomography. *Bioconjugate Chem.* **2016**, *27*, 170−178.
(55) Ge, Z. S.; Liu, S. Y. Functional block copolymer assemblies responsive to tumor and intracellular microenvironments for site-specific drug delivery and enhanced imaging performance. *Chem. Soc. Rev.* **2013**, *42*, 7289−7325.

DOI: 10.1021/acs.accounts.9b00080
Acc. Chem. Res. 2019, 52, 1485−1495

(56) Jeong, B.; Bae, Y. H.; Lee, D. S.; Kim, S. W. Biodegradable block copolymers as injectable drug-delivery systems. *Nature* **1997**, *388*, 860.
(57) Wang, C.; Stewart, R. J.; Kopeček, J. Hybrid hydrogels assembled from synthetic polymers and coiled-coil protein domains. *Nature* **1999**, *397*, 417−420.
(58) Gref, R.; Minamitake, Y.; Peracchia, M. T.; Trubetskoy, V.; Torchilin, V.; Langer, R. Biodegradable long-circulating polymeric nanospheres. *Science* **1994**, *263*, 1600−1603.
(59) Kataoka, K.; Harada, A.; Nagasaki, Y. Block copolymer micelles for drug delivery: design, characterization and biological significance. *Adv. Drug Delivery Rev.* **2001**, *47*, 113−131.
(60) Lee, C. C.; MacKay, J. A.; Frechet, J. M.; Szoka, F. C. Designing dendrimers for biological applications. *Nat. Biotechnol.* **2005**, *23*, 1517−1526.
(61) Ogris, M.; Brunner, S.; Schuller, S.; Kircheis, R.; Wagner, E. PEGylated DNA/transferrin-PEI complexes: reduced interaction with blood components, extended circulation in blood and potential for systemic gene delivery. *Gene Ther.* **1999**, *6*, 595−605.
(62) Huang, G.; Zhao, T.; Wang, C.; Nham, K.; Xiong, Y.; Gao, X.; Wang, Y.; Hao, G.; Ge, W.; Sun, X.; Sumer, B. D.; Gao, J. PET Imaging of Occult Malignancy by Chemical Integration of Tumor Acidosis. *Nat. Biomed. Eng.* **2019**, in press.

DOI: 10.1021/acs.accounts.9b00080
Acc. Chem. Res. 2019, 52, 1485−1495